Journal of Structural Geology, Vol. 11, No. 3, pp. 245 to 254, 1989
Printed in Great Britain

0191-8141/89 $03.00 + 0.00

Mathematical model for folding of layering near rigid objects in shear deformation

MARCIA BJORNERUD

Byrd Polar Research Center, The Ohio State University, Columbus, Ohio 43210, U.S.A.

(*Received* 25 *January* 1988; *accepted in revised form* 15 *September* 1988)

Abstract—The asymmetric arrangement of deformed layering around rigid objects in shear zones is among the most reliable criteria for inferring shear sense in rock. A mathematical model which simulates shear deformation of a ductile medium containing a rigid inclusion gives insight into the genesis of this type of shear sense indicator. The model, which is based on the velocity field solution for viscous flow around a sphere, demonstrates that many common strtuctures can arise in a mechanically passive matrix. As the model simulates increasing shear strain, structures in the matrix pass through distinct evolutionary stages. Similar results have been obtained in experimental models, suggesting that it may be possible to read shear strain magnitude from the geometry of deformed layering near clasts and porphyroclasts in sheared rocks.

INTRODUCTION

STRUCTURES observed around clasts and porphyroclasts in sheared rocks record interaction between the relatively rigid objects and ductile matrix during non-coaxial deformation. Previous theoretical studies of object–matrix interaction have focused on the object — either its motion (e.g. Ghosh & Ramberg 1976, Freeman 1985, Passchier 1987) or its change in shape (e.g. Gay 1968, Passchier & Simpson 1986) during sustained shear. The purpose of this study, in contrast, was to consider progressive deformation of the matrix enclosing the object.

The two-dimensional mathematical model presented here demonstrates that folding of layering near rigid objects in shear zones may be a largely passive process. Inspired by shear-related structures in a laminated diamictite, the model is based on a modified form of the velocity field solution for flow of a very viscous, homogeneous fluid around a sphere. In this paper, I discuss the design and results of the analytical model and compare its mathematically-simulated structures with natural and experimental counterparts.

MODEL DESIGN

Motivation for the model

The mesoscopic structural style of Upper Proterozoic diamictites in Wedel Jarlsberg Land, SW Spitsbergen, provided the stimulus for modeling object–matrix interaction during progressive shearing deformation. The matrix of the Kapp Lyell diamictites, which probably represents glaciomarine deposits (Waddams 1983), consists of centimeter-scale varve-like laminae. These laminae are clearly sedimentary; they are commonly graded and may represent influxes of clastic material carried by density currents into a generally quiet basin. The layering is visible because the upward decrease in grain size within individual laminae causes color contrasts between the top and bottom of each one. Pebble- to boulder-sized clasts, possibly ice-rafted dropstones, punctuate the otherwise fine-grained rocks.

Ductile thrusting during early Paleozoic ('Caledonian') tectonism caused overall layer-parallel shearing within the Proterozoic sequence of Wedel Jarlsberg Land (Bjornerud 1987). In thinly bedded cherty dolomites, a mylonitic foliation was developed parallel to bedding planes. Phyllitic layers in quartzite–argillite units acted as slip surfaces, accommodating large shear strains. In the Kapp Lyell diamictites, the geometry of deformation associated with the layer-parallel shear regime was strongly influenced by the clasts in the rocks.

Where clasts are absent or relatively small (diameters less than laminae thickness), the diamictites are characterized by strongly smeared or streaked layers, but few folds occur in the varve-like laminae (Fig. 1a). Where clasts are large and numerous, in contrast, the sedimentary layering is highly convoluted (Fig. 1b). In many cases, the convolutions in the layers are nucleated around clasts (Fig. 2). These apparently clast-induced folds resemble eddies downstream from obstacles in fluid flow. In the diamictites, the 'eddies' occur on both sides of clasts due to the shearing (rather than unidirectional) flow field, and the zones of disturbed layering commonly persist for 50–100 cm on either side of the clasts which seem to trigger them. Although a superficially similar geometry could be produced by coaxial flattening and crenulation of the layering, other meso- and microstructural features in the Kapp Lyell diamictites—e.g. transposed layering (Fig. 1b) and whorled pressure shadow fibers around pyrite crystals—support the interpretation of clast-related folds in the rocks as structures produced by non-coaxial deformation.

The eddy analogy for the diamictite structures must be

used with care because truly turbulent flow is precluded by the high viscosity (low Reynolds number *Re*) of deforming rock (Langlois 1964, Ghosh & Ramberg 1976). But the more general concept of an asperity causing instability in steady flow is valid for high viscosity media (Hudleston 1976, Cobbold & Quinquis 1980). With this in mind, I set out to determine whether the 'eddy' structures in the Spitsbergen diamictites could be mathematically replicated by allowing a passive, layered matrix to flow through a simple shear velocity field which was perturbed by the presence of a rigid inclusion.

Components of the model

The model's computer algorithm consists of two parts. In the first, local velocity vectors are defined at equally-spaced points in a grid which represents a shear-direction cross-section through the rigid object and ductile matrix (Fig. 4). In the second part of the program, points in this grid are allowed to 'flow' through the velocity field by iterative recalculation of their positions at small time increments. The results discussed in this paper were derived by holding the velocity field constant throughout the iterative process. Future experimentation with time-dependent velocity fields may be worthwhile.

The velocity field used in the model is the solution for low Reynolds number flow around a sphere, modified for simple shear (the necessary modifications are detailed below). The solution is based on the assumptions that the fluid matrix is homogeneous and isotropic and has no finite yield strength (Turcotte & Schubert 1982, p. 263). While these are, admittedly, restrictive assumptions which do not account for the mechanical non-uniformity inherent in a layered medium, this idealization of the system permits a purely kinematic analysis, obviating the need to assign absolute values for shear stress, strain rate and viscosity. (The viscosity is constrained only to the extent that $Re \ll 1$, so that inertial forces are negligible.) The model's generality is limited somewhat by use of the analytical velocity field solution, since it presupposes that the object in the fluid is spherical and undergoes no deformation. Many clasts in the diamictites not only had angular and non-equant original shapes, but also experienced deformation along with the enclosing matrix. Still, the simplified geometry of the model is reasonably accurate for the clasts around which the clearest 'eddies' occur and the results obtained for this geometry are useful and interesting.

The equations which define the velocity field for plane flow of a high-viscosity fluid past a sphere are:

$$u_r = U(-1 - a^3/(2r^3) + 3a/2r)\cos\theta \quad (1)$$

$$u_\theta = U(1 - a^3/(4r^3) - 3a/4r)\sin\theta \quad (\text{for } r > a) \quad (2)$$

in which a is the sphere radius; r and θ are polar co-ordinates centered on the sphere; u_r and u_θ are radial and tangential velocity components, respectively; and U is the far-field unidirectional flow velocity in the $\theta = 0$ direction (Turcotte & Schubert 1982, pp. 263–265).

The boundary conditions which constrain this solution are: (1) that the fluid approach a uniform velocity as r approaches infinity; and (2) that there be no slip at the boundary between the object and the fluid. (Because the object is considered stationary and not rotating, this means that $u_r = u_\theta = 0$ on $r = a$.) The perturbation velocity field depends only on the size of the sphere and the scaled flow rate.

To adapt the above velocity field for a shearing fluid, two changes are necessary. First, an ambient simple shear flow field must be substituted for the unidirectional far-field flow U. In the model's computer algorithm, velocity vectors are assigned sequentially to grid points by multiplying equations (1) and (2) by the vertical co-ordinate of each point so that the magnitude of the horizontal velocity component increases linearly with distance from the centerline. Second, in order to satisfy the no-slip boundary condition, the velocity of the edge of the sphere must equal the velocity of adjacent particles in the fluid. Because the sphere is assumed rigid, the no-slip condition means that the vorticity of the shear zone is partitioned into spin for points within the sphere (Lister & Williams 1983). The object will rotate at an angular velocity ω equal to half the bulk shear rate $\dot{\gamma}$ (Jeffrey 1922, Freeman 1985). For shearing flow, therefore, velocity vectors must be assigned at

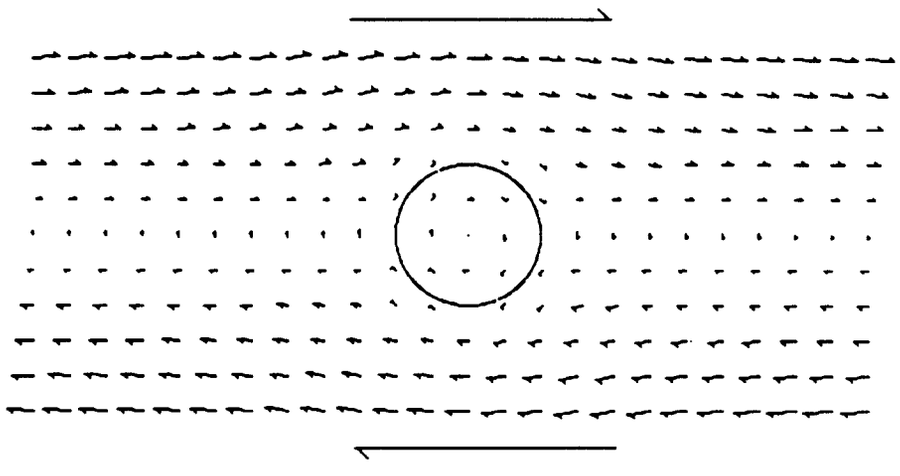

Fig. 4. Two-dimensional velocity field for viscous shearing flow around a rigid inclusion of circular cross-section.

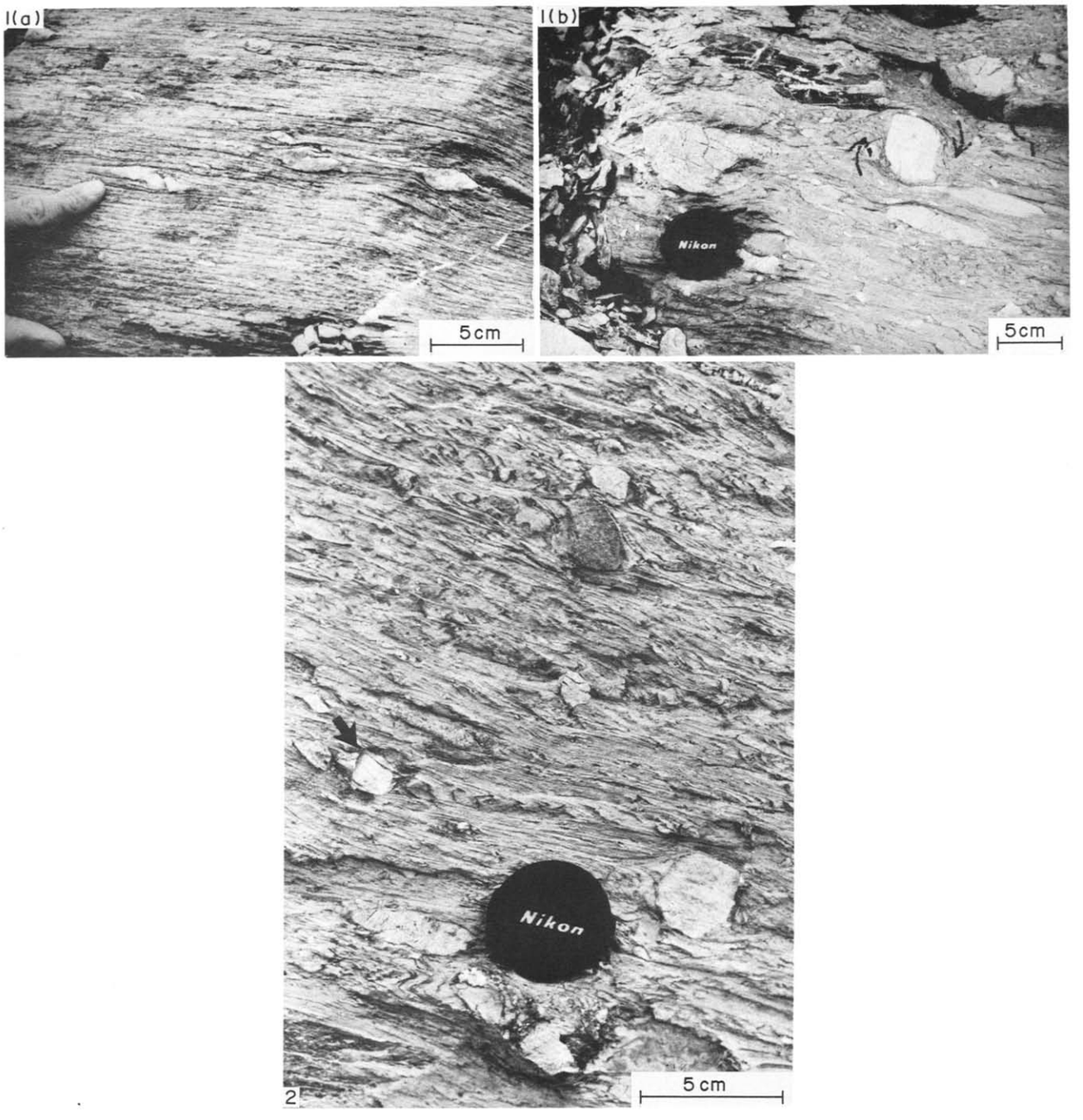

Fig. 1. Size, shape and abundance of clasts in Kapp Lyell diamictites controlled development of folds during layer-parallel shear. (a) Diamictite layering (approximately horizontal) is streaked but not folded where clasts are small and scattered. (b) Layering is complexly folded where clasts are large and closely spaced. Subhorizontal foliation in photograph is plane of shear. Layering, marked by fine dark bands at tops of 1–2 cm thick graded sequences, is generally at a large angle to shear surfaces. Folding of layering near white dolomite clast records dextral sense of rotation (arrows). In both photographs outcrop face is nearly vertical.

Fig. 2. White dolomite clast at center left (arrowed) locally disrupted simple shear flow field, causing layering to be folded in neighborhood of clast. Outcrop face is approximately vertical. Sense of shear is top to right.

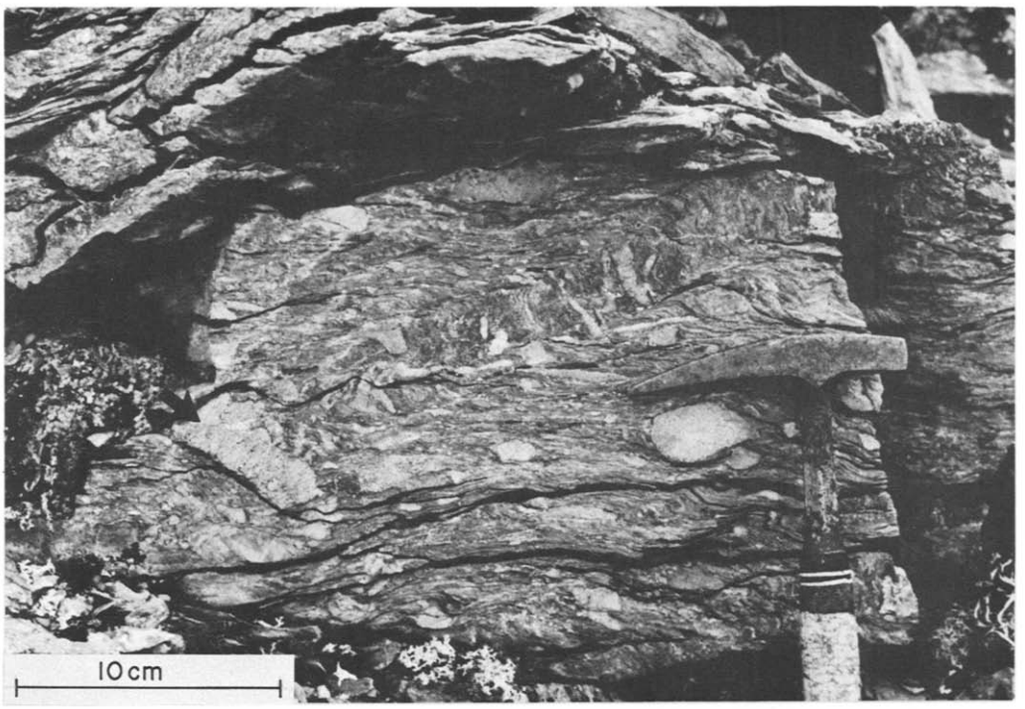

Fig. 3. Kink-like zone apparently nucleated by large quartzite clast at lower left. Overall sense of shear is top to right. See text for discussion.

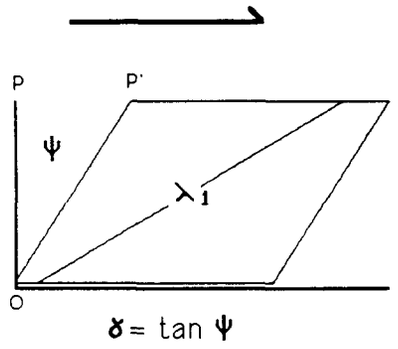

Fig. 5. Definitions of geometric variables in progressive simple shear. ψ = angular shear strain; γ = shear strain; λ_1 = maximum principal finite strain.

points inside the sphere, while the unidirectional flow solution prescribed velocities only outside the sphere. In the model's computer algorithm, the radial velocity u_r is set at 0 and the tangential velocity u_θ at ωr for all points where $r \leq a$, so that the sphere rotates about its center without deforming.

Once the program calculates the velocity field for a particular grid size and sphere radius (entered as input variables), simulated deformation occurs as originally rectilinear points are displaced by amounts proportional to the average magnitude of nearby velocity vectors. In order for the mathematical deformation process to approximate continuous natural deformation, the 'time' intervals between recalculations of grid point positions must be small enough that particles are not displaced through more than one grid interval in a given deformation increment. The bulk strain at any time is described by either the angular deflection ψ of an originally vertical line or by the tangent of this angle, γ (Fig. 5).

To represent finite deformation at specified intervals, the program generates two types of plots: (1) layering plots, in which points that lay on the same horizontal line before deformation are connected to show fold development; and (2) strain grid plots, which display the deformed shapes of originally square areas (Figs. 6, 7 and 9). In the next section, I discuss the features of some of these plots and compare them with their natural and experimental analogs.

MODEL RESULTS

The layering and strain plots produced by the model show a distinct sequence of structures which occur at progressively higher shear strains. However, the actual shear strain value at which a given structure is first visible depends on the size of the rigid object relative to the spacing of the marker lines. As object radius increases relative to layer thickness, the shear strain required to produce a particular feature decreases. An object with a radius smaller than the layer spacing will cause little distortion of the layering at any finite shear strain. Thus, assigning a shear strain value to a given structure is meaningful only if an object/layering ratio is specified. In the following discussion, I present results for object radii between one and three times the layer thickness. All plots included as figures are for object radii twice the layer thickness.

Evolution of folds and strain patterns in the matrix with increasing shear strain

At even very low shear strain, layering plots generated by the model show asymmetric half-folds in the matrix close to the object (Fig. 6a). The folds are convex in the

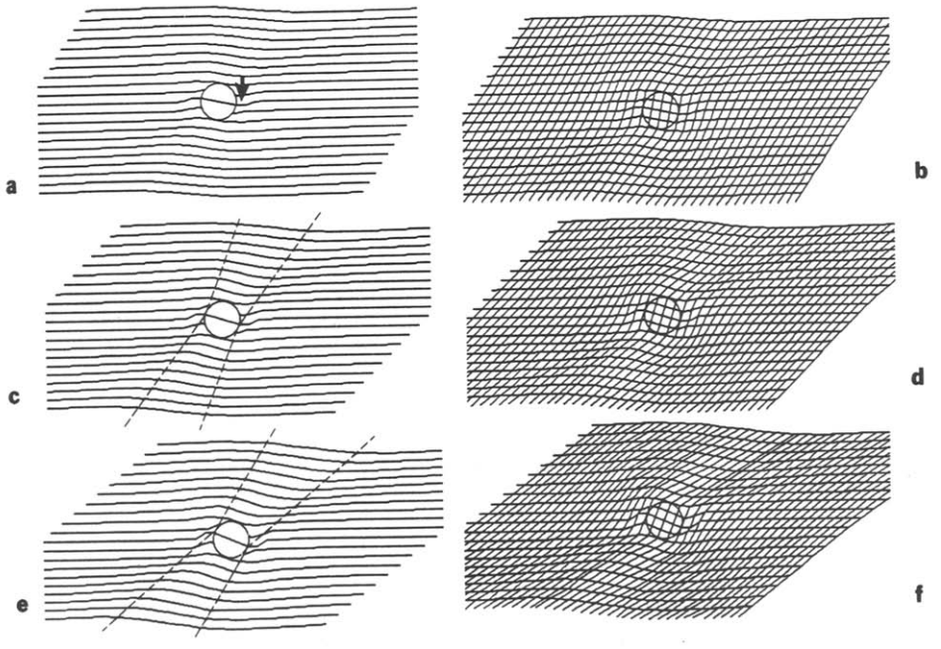

Fig. 6. Model plots for low shear strain. Parts (a), (c) and (e) show deformation of layering at shear strains γ = 0.69, 1.03 and 1.37, respectively; (b), (d) and (f) show corresponding distortion of originally rectilinear grid at same finite shear strains. Arrow in (a) points to asymmetric half-fold near object. As shear strain increases, amplitude of such folds grows, and thickness of limbs decreases. Dashed lines in (c) and (e) mark boundaries of flexed zones.

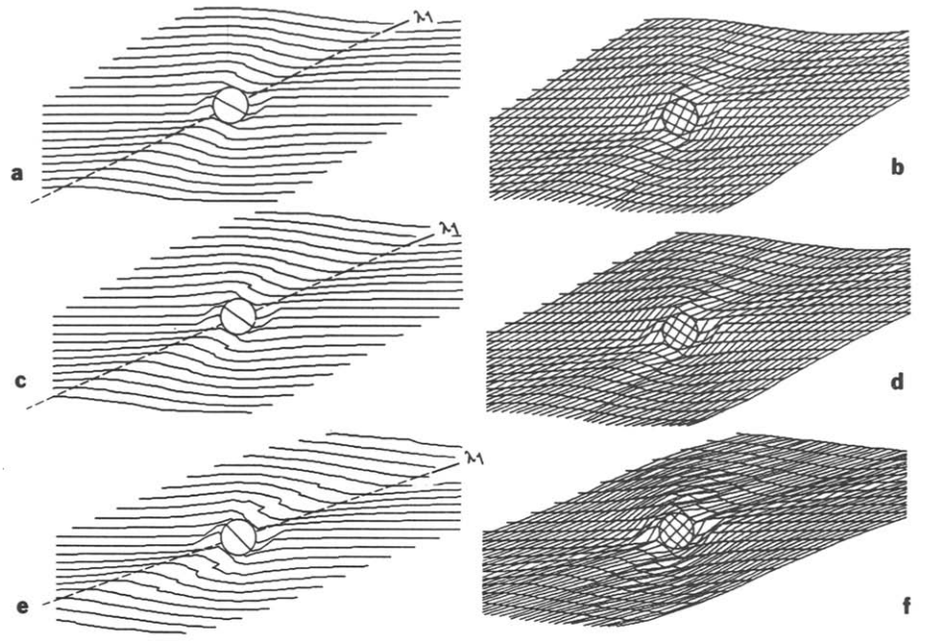

Fig. 7. Layering and grid plots for intermediate shear strain. Plots (a) and (b) were produced at $\gamma = 1.67$; (c) and (d) at $\gamma = 1.99$; (e) and (f) at $\gamma = 2.72$. Dashed lines mark band of thinned layering and maximum principal finite strain direction (λ_1).

direction of the object's rotation, and they form as the rotating object pulls the adjacent matrix with it, a consequence of the no-slip condition at the object–matrix boundary (Ghosh & Ramberg 1976, Schoneveld 1977). As a further result of the no-slip constraint, marker spacing is decreased in the limbs of the folds (Fig. 6b). This reflects the decreasing importance of spin relative to shear-induced vorticity in the matrix away from the object.

Folds and thinned layering are familiar features near clasts and porphyroclasts in natural shear zones, and the asymmetry of such features is one of the most useful criteria for inferring shear sense in deformed rock (Simpson & Schmid 1983). Mathematical simulation of these features by the simple kinematic fluid model indicates that they can develop without dynamic behavior by the layering. The folds simply reflect the constraint of no differential movement between object and matrix.

As shear strain increases, the object continues to rotate. The half-folds in layers next to the object grow in amplitude, and the layer spacing in the fold limbs decreases further (Fig. 6c). At the same time, open folds become visible in layers away from the object, their amplitudes decreasing to zero at a radial distance of several diameters. The inflection points of these gentle folds define the boundaries of warped or flexed zones above and below the object (Figs. 6c & e). Within these zones, layer spacing is slightly increased (Figs. 6d & f). The flexure boundaries are slightly non-parallel, diverging away from the object, but the flexed zones as a whole are oriented in the direction of the deflected perpendicular (OP' in Fig. 5).

This gentle flexure of the layering is an ephemeral feature in the evolution of the shear zone. It reflects the parallelism of velocity vectors with layering in the areas directly above and below the object at low shear strain. With continued shear, the flexed zones move into positions where velocity vectors no longer coincide with layering. The layers within the zones become deformed and lose their approximate parallelism. The transitory nature of the simple flexed zones makes them potentially useful as indicators of strain magnitude in natural shear zones. For the idealized geometry of the model and an object radius twice the layer thickness, layers within the flexed zones remain subparallel only until the bulk shear strain γ reaches about 2. For larger objects, layers within the zones deform at lower shear strains.

Figure 3 shows a possible natural example of a clast-nucleated flexure zone in the Proterozoic diamictites of SW Spitsbergen. The geometry and mechanical behavior of this natural system, however, are clearly more complex than those of the model. The large quartzite clast seems to have rotated rigidly while smaller clasts have deformed plastically (several are themselves bent into the flexed zone). The shapes of the smaller clasts within the flexed zone also suggest that they underwent deformation before the zone developed, so the finite shear strain in this case may be higher than the geometry of the flexed zone would suggest. Smaller apparently clast-nucleated folds in the photograph indicate more advanced stages of shear.

When the flexed zones have been translated out of their original positions above and below the object, the zones enter a part of the velocity field where there is a significant component of motion perpendicular to the shear zone boundaries, and the result is the development of small folds in the flexed layering (Figs. 7a & c). The asymmetry of these folds is consistent with the bulk sense of shear.

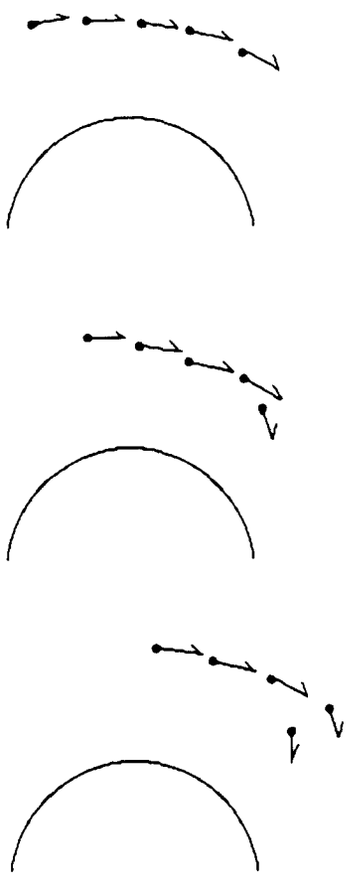

Fig. 8. Development of an isoclinal fold in a single layer as a leading particle is overridden by trailing particles on downshear side of object. Arrows represent velocity vectors which govern movement of particles in next time increment.

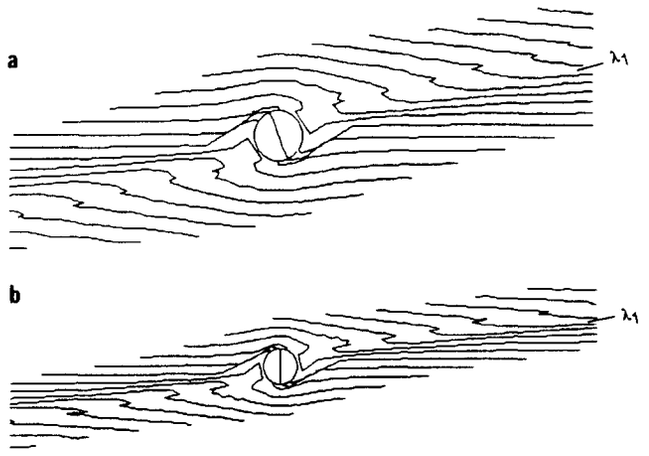

Fig. 9. Layering plots for high shear strain. In (a) $\gamma = 4.32$ and in (b) $\gamma = 5.92$.

Figure 8 traces the development of one such fold in a layer in the upper half of a dextral shear zone. The layering from the flexed region is tilted in the downshear direction as it moves to the right out of its original position. The tilting occurs because the layer's leading particles encounter velocity vectors with relatively large components perpendicular to the shear direction (downward in Fig. 8), while the trailing particles meet vectors which are only slightly oblique to the shear direction (horizontal and toward the right). The differential vertical motion between leading and trailing particles progressively steepens the layering until a downward-moving leading particle is overridden by a trailing particle, forming a small flap. At the critical shear strain, small folds of this type form almost simultaneously in layers up to several radii away from the object (Fig. 7a & c). With increasing strain, new folds develop farther out in the matrix (Fig. 7e).

It is instructive to consider not only the evolution of these folds but also the positions of individual particles within them. Layers close to the rotating object are caught permanently in its vortex. Therefore, as deformation progresses, new particles are dragged into the folds. Particles migrate through the hinge positions of the folds, and segments of the layers are first compressed then stretched — in effect unstrained — as they move into positions of extensional incremental strain, in the manner described by Ramsay *et al.* (1983). Such 'unstraining' is less obvious two or more layers away from the object, where essentially the same material point occupies a given fold hinge from the time the fold develops through progressively higher states of shear strain. This probably reflects the fact that folds in the far field are translated into regions of nearly homogeneous simple shear deformation, and continued shear of the relatively tight folds serves only to magnify their amplitudes.

At about the same time that the flap-folds develop in the matrix, a narrow band of closely-spaced layering becomes increasingly visible (Fig. 7c). This band is parallel to the maximum finite elongation (λ_1) direction associated with the bulk shear strain. In the layer plots, the band bears a superficial resemblance to a shear band, but this is inconsistent with its orientation parallel to a principal strain axis. Rather, the band develops as the downshear boundaries of the early flexed zone are rotated and flattened.

With continued shear, the features developed at lower shear strains are themselves passively deformed. In the near field, layers controlled by the no-slip condition continue to curl around the object. The limbs of these curling folds, already strongly attenuated, undergo further thinning and stretching. Away from the object, the amplitude of the tight flap-folds increases, while the enveloping surfaces of the folds rotate toward the shear zone boundaries. The band of closely-spaced layering, parallel to the fold packet, also rotates towards the shear plane (Fig. 9). The clast-nucleated structure shown in Fig. 2 appears to represent an advanced state of shear strain in which both the band of appressed layering and the fold envelope lie virtually parallel to the shear plane.

Summary of model results

The following structures appear in sequence as the model simulates increasing shear strain:

(1) asymmetric half-folds with thinned limbs, formed next to the object as a result of its spin vorticity and the no-slip condition between object and matrix;

(2) flexed zones of thickened layering immediately above and below the object, reflecting the temporary parallelism of velocity vectors and layering in those positions at low shear strain;

(3) flap-folds, developed when adjacent particles undergo differential displacement perpendicular to the shear direction;

(4) narrow bands of closely-spaced layering, oriented in the maximum principal strain direction and formed by rotation and flattening of the flexed-zone boundaries.

Recognizing the sequential development of these features is a first step toward a set of criteria for estimating shear strain magnitude in natural shear zones.

Comparison of computer-generated structures with experimental models

Experimental simulations of ductile matrix–rigid object interaction during layer-parallel shear have been conducted recently by Passchier & Simpson (1986) and Van den Driessche & Brun (1987). In both studies, a passive silicone matrix was allowed to flow around a rigid object. Passchier & Simpson (1986), who were concerned mainly with the evolution of recrystallized tails around large crystals during shear, used rigid cylinders of progressively smaller diameter to simulate the development of a strain-softened mantle on a porphyroclast with increasing shear strain. Van den Driessche & Brun (1987) conducted a set of experiments for a rigid object of constant size with no recrystallized mantle, and these experiments correspond most closely to the mathematical model presented in this paper.

In the scale models of Van den Driessche & Brun, the rigid object was rectangular in cross-section, with an aspect ratio of 2:1 and the smaller dimension equal to about twice the layer thickness. This shape was chosen as an approximation for a typical feldspar porphyroclast. Despite the difference in object shape, the 'rolling structures' produced in the physical models passed through the same evolutionary stages as the mathematically-simulated structures. And because the relative sizes of the objects in the experimental and computer models were comparable, so were the bulk shear strains at which the various structures appeared.

Van den Driessche & Brun (1987) focused primarily on features generated at high shear strain and thus did not discuss in detail structures developed at the onset of shearing deformation. However, a sketch showing layer deformation at $\gamma = 1.2$ (their fig. 11a) displays several characteristics of the low-γ computer plots. Next to the object, there are small half-folds, convex in the rotation direction. Above and below the object, layering is flexed and slightly thickened. The flexed zone is relatively narrow, probably because the object was oriented with its long axis perpendicular to layering at the beginning of deformation.

By a finite shear strain of $\gamma = 3.8$, tight folds and oblique bands of thinned layering have appeared in the experimental models (see fig. 11b of Van den Driessche & Brun 1987). As in the computer-generated plots, the bands are parallel to the maximum principal strain axis for the shear zone as a whole. Like the bands in the computer plots, they might be mistaken for shear bands. However, the shapes of strain markers imprinted on the silicone matrix show that the bands are not shear planes but passively amplified warps in the layering (Van den Driessche & Brun 1987).

The tight folds formed at moderate shear strain in the physical models are significantly larger in amplitude than those in the corresponding computer plots. This probably reflects differences in the velocity field set up by the sphere in the computer model and the oblong, sharp-cornered object in the physical experiments. The symmetry of a sphere keeps the velocity field constant with respect to a fixed (Eulerian) co-ordinate system as the object rotates. For a less symmetric shape like a rectangle, however, the Eulerian velocity vectors are constantly changed as the object rotates and its unequal sides meet the shear flow at varying angles. It follows that the shapes and amplitudes of folds generated by the rotation of an inequant object will depend partly on the object's initial position. In addition, the corners of such an object may induce local velocity disturbances. These factors may contribute to the relatively large amplitudes of folds in the experimental models.

With further increases in shear strain, structures in the scale models evolve in much the same way as their computer-simulated counterparts. Layering in the oblique bands becomes more attenuated, existing folds grow in amplitude, and new folds develop in layers progressively farther from the object (see figs. 9 and 11 of Van den Driessche & Brun 1987).

Based on their experimental observations, Van den Driessche & Brun suggested that the length of the fold packet (normalized for the object dimensions) is proportional to shear-strain magnitude. In the computer model, rising shear strain did cause a general increase in the extent of the folds, but an exact proportionality was difficult to establish. At the critical shear strain, in fact, folds appeared simultaneously in layers up to several diameters away from the sphere (Figs. 7a & c). This difference between the two models may be related to the fact that time and space are discretized in the mathematical model but continuous in the physical model.

A phenomenon common to both models is the local unstraining of areas near the object as material points migrate through the hinge zones of amplifying folds. As Van den Driessche & Brun (1987) point out, the strain ellipses on the silicone matrix of their model illustrate this deformation reversal. The relatively large amplitude of the folds in the physical model may enhance the effect.

Aside from minor differences arising from model design, the physical and mathematical simulations of a rigid object in a ductile shear zone yield similar results. In each case, the shearing matrix induces the object to rotate, while the rotating object causes the passive matrix to deform. Distinct deformational features occur sequentially in the matrix as shear strain increases.

CONCLUSIONS AND REMAINING QUESTIONS

An attempt to explain the morphology of folds near clasts in a layered diamictite has led to the following conclusions.

(1) Shear deformation of a ductile material containing a rigid object is analogous to flow of a very viscous fluid around an obstruction. Structures observed close to rigid objects in both natural and experimental shear zones can be simulated mathematically by allowing a passive layered matrix to move through the analytically-derived velocity field for flow around a sphere.

Although this velocity field remains constant with respect to a fixed (Eulerian) reference frame during deformation, the velocity field in the (Lagrangian) reference frame of the matrix particles is time-dependent, making the flow unsteady (Malvern 1969, pp. 138–145). Folds in the passive layering develop as a result of this flow unsteadiness in the manner described by Hudleston (1976).

(2) The simple mathematical model for interaction between the ductile matrix and rigid object generates a characteristic succession of structures as shear strain increases. In order of appearance these include: (a) asymmetric half-folds next to the object; (b) warped or flexed zones above and below the object; (c) tight folds which amplify with increasing shear; and (d) bands of thinned layering which parallel the maximum principal stretch direction. A similar succession of structures has been observed in experimental models. The purely kinematic nature of the model presented here makes it applicable to a variety of rigid object–ductile matrix systems — not only to clasts in diamictites and porphyroclasts in mylonites, but also to phenocrysts in banded rhyolite flows (Vernon 1987) and cobbles incorporated into flowing ice or unlithified layered sediments. Although variables other than finite shear strain (e.g. object size and shape) influence the development of object-nucleated structures, mathematical simulation of their progressive evolution suggests their potential utility as indices of relative shear strain magnitude.

Remaining questions

Although the computer model presented in this paper gives insight into the genesis of shear-related structures around rigid objects, it raises many other questions about the development of these structures.

First, the mechanical role of layering in natural shear zones must be better understood before shear strain can be read systematically from naturally occurring structures. The very existence of layering in a rock precludes totally passive matrix behavior during deformation; the mineralogical contrasts which define the layers imply some contrast in dynamic properties. For that matter, these dynamic contrasts are probably responsible for setting up layer-parallel shear flow in the first place. So completely passive layer behavior seems unlikely in a shearing rock.

Mechanically active layering may either damp or amplify the velocity perturbations induced by the presence of a rigid object in a ductile shearing matrix. In the case of the Spitsbergen diamictites, the persistence of 'eddy' structures tens of centimeters from nucleating clasts (Fig. 2) may reflect some dynamic amplification by the varve-like laminae. If the diamictites are glaciogenic, an original 'dropstone' fabric with layering deflected around the clasts might also have accentuated the flow perturbation due to the rigid clasts themselves. On the other hand, the fact that 'eddies' are not more common in sheared layered rocks suggests that development of the structures is sometimes inhibited by the strength of the matrix layering. Why damping occurs in some instances and amplification in others is a question for future study.

Another potentially fruitful direction for analysis is consideration of the third dimension, since it seems unlikely that shearing flow would remain planar in the vicinity of an obscuring object. Decay of the velocity perturbation in the third dimension would probably give rise to sheath folds (Cobbold & Quinquis 1980). Localized fold trains without any obvious nucleating objects are common in sheared rocks and are often identified as 'shear bands', but some of these convolutions might be shear-perturbation features induced by objects which are not in the plane of observation. Finally, closely spaced clasts or porphyroclasts might set up three-dimensional flow disturbances with complex interference patterns, generating confusing structural geometries in which essentially coeval folds cross-cut each other.

Acknowledgments—This work was supported by the Byrd Postdoctoral Fellowship at the Byrd Polar Research Center, Ohio State University. Field work on Spitsbergen was funded by National Science Foundation grant DPP-8203038 to Professor Campbell Craddock at the University of Wisconsin-Madison. I wish to thank Richard Alley and Chris Mawer for helpful discussions. The comments of Peter Hudleston, Terry Wilson and two anonymous reviewers significantly improved the manuscript.

REFERENCES

Bjornerud, M. 1987. Structural evolution of a Proterozoic metasedimentary terrane, Wedel Jarlsberg Land, SW Spitsbergen. Unpublished Ph.D. thesis, University of Wisconsin-Madison.

Cobbold, P. & Quinquis, H. 1980. Development of sheath folds in shear regimes. *J. Struct. Geol.* **2**, 119–126.

Freeman, B. 1985. The motion of rigid particles in slow flows. *Tectonophysics* **34**, 163–183.

Gay, N. 1968. Pure shear and simple shear deformation of inhomogeneous viscous fluids. 1. Theory. *Tectonophysics* **5**, 211–234.

Ghosh, S. & Ramberg, H. 1976. Reorientation of inclusions by a combination of pure and simple shear. *Tectonophysics* **34**, 1–70.

Hudleston, P. 1976. Recumbent folding in the base of the Barnes ice cap, Baffin Island, NW Territories, Canada. *Bull. geol. Soc. Am.* **87**, 1684–1692.

Jeffrey, G. 1922. The motion of ellipsoidal particles immersed in a viscous fluid. *Proc. R. Soc. Lond.* **A102**, 161–179.

Langlois, W. 1964. *Slow Viscous Flow*. Macmillan, New York.

Lister, G. & Williams, P. 1983. The partitioning of deformation in flowing rock masses. *Tectonophysics* **92**, 1–33.

Malvern, L. 1969. *Introduction to the Mechanics of a Continuous Medium*. Prentice-Hall, Englewood Cliffs, New Jersey.

Passchier, C. 1987. Stable positions of rigid objects in non-coaxial flow — a study in vorticity analysis. *J. Struct. Geol.* **9**, 679–690.

Passchier, C. & Simpson, C. 1986. Porphyroclast systems as kinematic indicators. *J. Struct. Geol.* **8**, 831–843.

Ramsay, J., Casey, M. & Kligfield, R. 1983. Role of shear in development of the Helvetic fold-thrust belt of Switzerland. *Geology* **11**, 439–442.

Schoneveld, C. 1977. A study of some typical inclusion patterns in strongly paracrystalline-rotated garnets. *Tectonophysics* **39**, 453–471.

Simpson, C. & Schmid, S. 1983. An evaluation of criteria to deduce the sense of movement in sheared rocks. *Bull. geol. Soc. Am.* **94**, 1281–1288.

Turcotte, D. & Schubert, G. 1982. *Geodynamics: Applications of Continuum Physics to Geological Problems*. John Wiley and Sons, New York.

Van den Driessche, J. & Brun, J.-P. 1987. Rolling structures at large shear strain. *J. Struct. Geol.* **9**, 691–704.

Vernon, R. 1987. A microstructural indicator of shear sense in volcanic rocks and its relationship to porphyroblast rotation in metamorphic rocks. *J. Geol.* **95**, 127–133.

Waddams, P. 1983. Late Precambrian resedimented conglomerates from Bellsund, Spitsbergen. *Geol. Mag.* **120**, 154–164.